Juvenile Huntington Disease: CT and MR Features

Vincent B. Ho, H. Sylvester Chuang, Miguel J. Rovira, and Betty Koo

PURPOSE: To describe the clinical and radiologic manifestations of juvenile Huntington disease and to determine whether adult imaging criteria for Huntington disease are helpful for pediatric patients. **METHODS:** Six patients (3 to 18 years of age; mean age, 9.8 ± 5.6 years; 3 female, 3 male) with juvenile Huntington disease were studied with CT (n = 6) and/or MR (n = 3). CT and MR studies were evaluated for frontal horn distance/intercaudate distance and bicaudate ratios, which were compared with those of 24 age-matched healthy children and 12 age-matched patients with Leigh (n = 9) or Wilson (n = 3) disease. **RESULTS:** Atrophy of the caudate nuclei was identified in all Huntington patients. The frontal horn distance/intercaudate distance (1.64 ± 0.39) and bicaudate (0.205 ± 0.060) ratios of the patients with juvenile Huntington disease were found to be significantly different from those of healthy children and that of those patients with Leigh/Wilson disease. The 3 patients with Huntington disease who underwent MR evaluation were noted to have increased proton density– and T2-weighted signal in the caudate nuclei and putamina. **CONCLUSION:** As in adult patients, the use of frontal horn distance/intercaudate distance and bicaudate ratios are helpful for the diagnosis of Huntington disease in pediatric patients. On MR, increased proton density– and T2-weighted signal in the atrophic caudate nuclei and putamina are additional features of juvenile Huntington disease.

Index terms: Huntington disease; Pediatric neuroradiology

AJNR Am J Neuroradiol 16:1405–1412, August 1995

Huntington disease (HD) is a hereditary neurodegenerative disorder with a worldwide prevalence of 5 to 10 per 100 000 persons (1, 2). Typically, patients with HD present during adulthood (30 to 40 years of age) with choreoathetoid movements ("Huntington chorea"), progressive dementia, and behavioral disturbance. However, 1% to 6% of HD patients will have childhood onset (3–5). Unlike adult HD, juvenile HD patients more commonly present with cerebellar symptoms, dyslalia, mental deterioration, seizures, "parkinsonlike" rigidity, and hypokinesis. Chorea, characteristic for adult HD, seldom is evident initially in the juvenile HD form, frequently making the clinical diagnosis of juvenile HD elusive until late in its course (3–10).

The main radiologic feature of HD is that of caudate atrophy, which has been described on pneumoencephalography (4, 7, 11–12), computed tomography (CT) (10, 13–20) and magnetic resonance (MR) imaging (21–24). Caudate atrophy can be quantified by the use of ratios that compare the intercaudate distance (CC) to other internal standards (Fig 1)—most commonly, frontal horn (FH) width and calvarial width (inner table [IT]). In HD, there is an increase in CC out of proportion to FH or IT, which results in a decrease in the FH/CC ratio and an increase in the CC/IT ratio (bicaudate ratio). These criteria, however, have been established primarily from adult data. The radiologic descriptions of juvenile HD remain sparse (4, 7, 10, 24). We report the clinical and radio-

Received September 27, 1994; accepted after revision February 10, 1995.

From the Department of Radiology, Madigan Army Medical Center, Tacoma, Wash (V.B.H., M.J.R.); the Departments of Radiology (H.S.C.) and Neurology (B.K.), Hospital for Sick Children, Toronto, Ontario, Canada; the Department of Radiology, University of Washington, Seattle (V.B.H., M.J.R.); and the Department of Radiology, Oregon Health Sciences University, Portland (V.B.H.).

The opinions or assertions contained herein are the private views of the authors and are not to be construed as official or reflecting the views of the Department of the Army or of the Department of Defense.

Address reprint requests to Vincent B. Ho, MD, Department of Radiology, Attn: MCHJ-R, Madigan Army Medical Center, Tacoma, WA 98431-5000.

AJNR 16:1405–1412, Aug 1995 0195-6108/95/1607–1405
© American Society of Neuroradiology

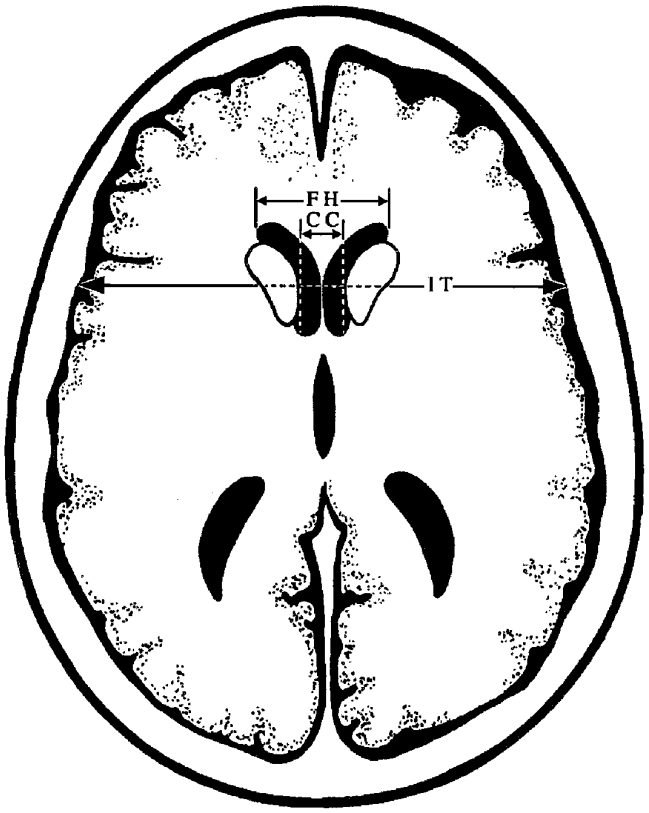

Fig 1. Schematic diagram of an axial projection at the level of the heads of the caudate nuclei at which the intercaudate distance (CC), the frontal horn (FH) width, and calvarial inner table (IT) width can be measured. The IT is measured at the same coronal level as the CC.

logic features of juvenile HD and investigate the use of adult imaging criteria for the diagnosis of HD in children.

Subjects and Methods

The six pediatric patients with HD ranged from 3 to 18 years old (mean age, 9.8 ± 5.6 years). Three patients were female, three male. The duration of clinical follow-up ranged from 6 months to 11 years. A summary of each patient's clinical features is provided in Table 1. All six patients manifested a combination of cerebellar symptoms (6 of 6), dyslalia (5 of 6), mental deterioration (5 of 6), rigidity (5 of 6), chorea (4 of 6), and/or seizures (4 of 6). Cerebellar symptoms (6 of 6), dyslalia (4 of 6), mental deterioration (3 of 6), and seizures (2 of 6) were the most common initial presenting symptoms. Chorea was evident in only one patient as a presenting symptom. All six patients had extensive family histories of HD, many of whom had early onset between 20 and 30 years of age. Four patients had paternal lines of inheritance; two patients, maternal.

The first comparison group comprised 24 healthy children (1 to 18 years of age; mean age, 8.75 ± 4.9 years; 12 female, 12 male) who had undergone CT examination for suspected trauma but had had (*a*) a normal head CT and (*b*) an uneventful postexamination course. The second comparison group comprised 12 pediatric patients (mean age, 7.96 ± 6.0 years) without HD who had bilateral basal ganglia abnormalities on CT and/or MR (Fig 4). Leigh disease was diagnosed in 9 patients, based on characteristic neuroimaging findings, clinical presentation, and metabolic alterations (including lactic acidosis, elevated serum and/or cerebrospinal fluid lactate/pyruvate ratios, and biochemical defects in pyruvate metabolism). In the 3 remaining patients of the second group, Wilson disease was diagnosed clinically (Kayser-Fleischer rings, decreased serum ceruloplasmin, elevated urinary copper) in 2 children. Liver biopsy was required to confirm the diagnosis of Wilson disease in the remaining child.

Six CT and three MR examinations were performed on the six patients with juvenile HD. CT scans were obtained on GE 8800 or GE 9800 Quick Highlight CT scanners with axial contiguous 5- or 10-mm section thickness and a 320 × 320 matrix. MR evaluations were performed on a 1.5-T GE Signa scanner using T1 (500-700/20/2 [repetition time/echo time/excitations]), proton density (2400-2800/30/1), and T2 (2400-2800/70-80/1) pulse sequences. Sagittal and axial T1-weighted and axial proton-density and T2-weighted images were obtained. In two patients, coronal images also were obtained.

Three measurements were obtained on axial images at the level of the third ventricle (Fig 1): (*a*) the FH width, representing the distance between the most lateral aspects

TABLE 1: Clinical features of juvenile Huntington patients

Case	Age of Onset, y	Cerebellar Symptoms	Dyslalia	Mental Deterioration	Rigidity	Chorea	Seizure	Family History
1	3	++	+	+	+	+	+	m
2	4½	++	++	+	+	+	+	p
3	8	++	++	++	+	−	++	m
4	13½	++	++	++	+	+	−	p
5	9½	++	++	++	−	−	−	p
6	8	++	−	−	+	++	++	p

Note.—+ indicates presence of symptom; ++, presenting symptom; −, absence of symptom; m, maternal inheritance; and p, paternal inheritance.

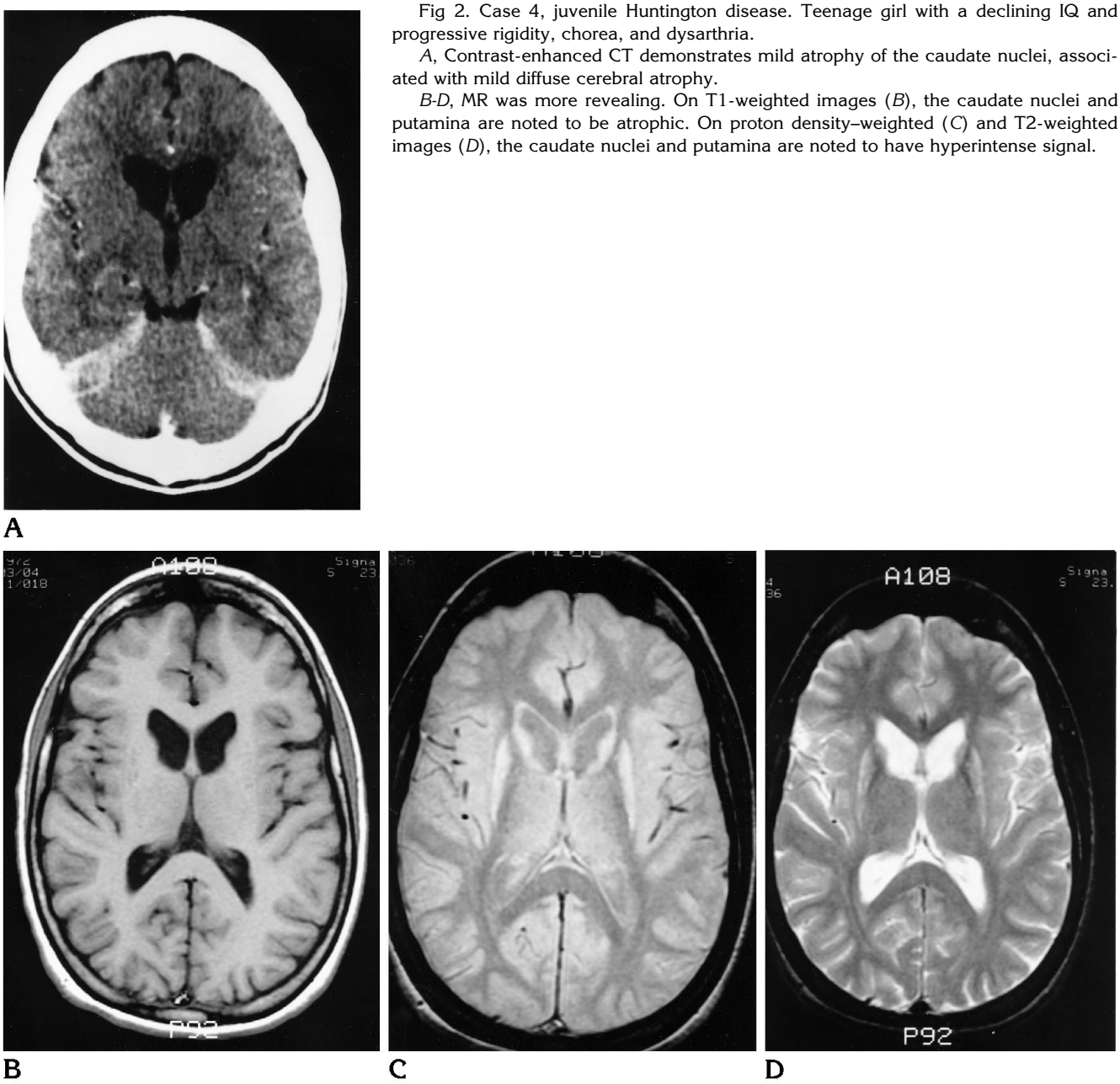

Fig 2. Case 4, juvenile Huntington disease. Teenage girl with a declining IQ and progressive rigidity, chorea, and dysarthria.

A, Contrast-enhanced CT demonstrates mild atrophy of the caudate nuclei, associated with mild diffuse cerebral atrophy.

B-D, MR was more revealing. On T1-weighted images (*B*), the caudate nuclei and putamina are noted to be atrophic. On proton density–weighted (*C*) and T2-weighted images (*D*), the caudate nuclei and putamina are noted to have hyperintense signal.

of the frontal horns; (*b*) the intercaudate distance (CC), the distance between the most medial aspect of the caudate nuclei; and (*c*) the IT width, the distance between the inner tables of the calvarium at the level of the CC measurement. The FH, CC, and IT measurements then were used to calculate the FH/CC and bicaudate (CC/IT) ratios (13–20, 23). The FH/CC and bicaudate ratios then were compared with those measured from (*a*) CT examinations from 24 age-matched healthy children and (*b*) CT and MR exams from 12 age-matched patients with Leigh or Wilson disease. All measurements and film interpretations were made by at least two neuroradiologists.

Results

All six children with HD were noted to have caudate atrophy by CT (Fig 2A) and/or MR (Figs 2B–D and 3A–C) associated with diffuse cerebral atrophy. Atrophy of the putamina was identified in all patients who had MR performed (Figs 2B–D and 3A–C). Abnormal high signal was noted in the caudate nuclei and putamina bilaterally on proton density–weighted (Figs 2C and 3B) and T2-weighted (Figs 2D and 3C) images in all three patients who underwent MR

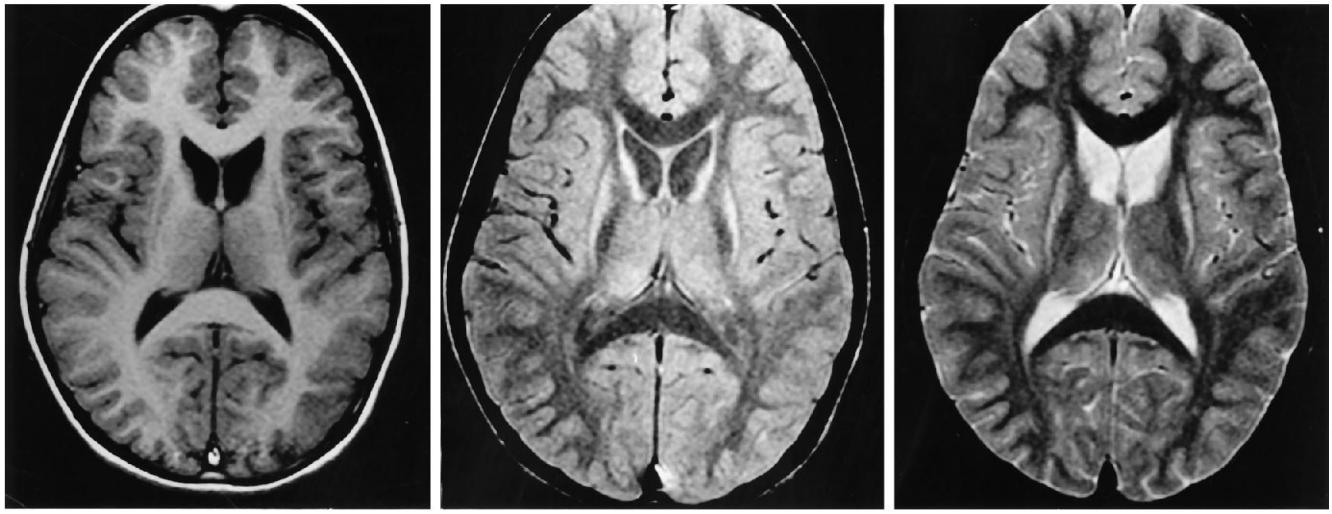

Fig 3. Case 6, juvenile Huntington disease. The patient is an 8-year-old boy who has a newly diagnosed seizure disorder and balance difficulties. The caudate nuclei and putamina are noted to be atrophic on T1-weighted images (*A*) and to have increased signal intensity on proton density–weighted (*B*) and T2-weighted (*C*) images.

evaluation. The results of the six CT and three MR examinations on our six pediatric patients with Huntington disease are summarized in Table 2. The corresponding FH/CC and bicaudate ratios for the three groups (juvenile HD, healthy children, and patients with Leigh/Wilson disease) are graphically represented in Figures 4 and 5, respectively. Analysis of variance was performed for all three groups to determine statistical differences. There was a statistically significant difference between the FH/CC ratio of juvenile HD patients (mean FH/CC ratio, 1.64 ± 0.39) and that of healthy children (mean FH/CC ratio, 3.82 ± 1.36; $P = .0068$) and that of children with Leigh or Wilson disease (mean FH/CC ratio, 4.62 ± 3.27; $P = .0013$). Similarly, the bicaudate ratio of juvenile Huntington patients (mean bicaudate ratio, 0.205 ± 0.060) also was found to be statistically different from that of healthy children (mean bicaudate ratio, 0.093 ± 0.068; $P < .0001$) and Leigh/Wilson patients (mean bicaudate ratio, 0.105 ± 0.067; $P = .0013$). No statistical differences in either FH/CC ($P = .255$) or bicaudate ratio ($P = .635$) were found between the comparison groups (healthy children and Leigh/Wilson patients).

Discussion

HD is an autosomal dominant neurodegenerative disorder that typically presents during

TABLE 2: Radiologic features of juvenile Huntington patients

Case	Imaging	Age, y	Duration of Symptoms, y	FH/CC Ratio	Bicaudate Ratio	Diffuse Cerebral Atrophy	MR Features*
1	CT	3	½	2.25	0.136	none	
	CT	5	2½	2.20	0.138	none	
	CT	7	4½	1.30	0.301	severe	
2	CT	5	1	1.87	0.163	moderate	
3	CT	17	11	1.29	0.246	moderate	
4	CT	15½	2½	1.39	0.253	mild	
	MR	18	5	1.32	0.253	mild	−T1, ↑PD, ↑T2
5	MR	9½	1	1.75	0.161	mild	−T1, ↑PD, ↑T2
6	MR	8	½	1.37	0.195	mild	−T1, ↑PD, ↑T2

Note.—* MR features of the caudate nuclei and putamina on T1-, proton density (PD)– and T2-weighted images were either isointense (−) or hyperintense (↑).

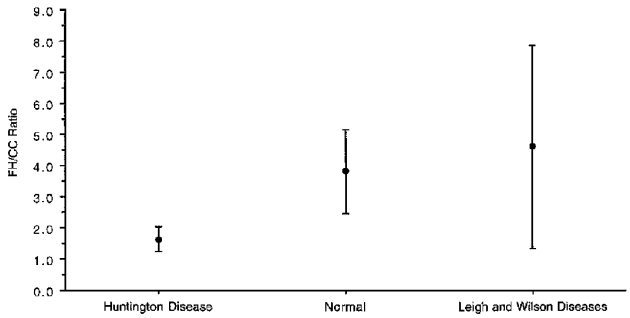

4

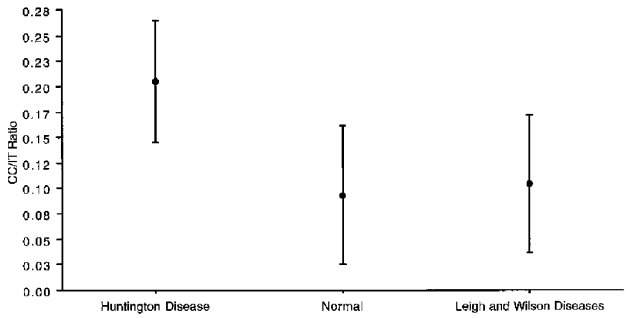

5

Fig 4. Ratios of frontal horn distance to intercaudate distance for children with Huntington disease, healthy children, and children with Leigh or Wilson diseases.

Fig 5. Bicaudate ratios (intercaudate distance to inner table width) for children with Huntington disease, healthy children, and children with Leigh or Wilson diseases.

adulthood but occasionally may manifest during childhood (1, 4, 6, 25, 26). HD has a wide variation in its age of onset even within a single family. Although there is no clear sexual predilection for HD, there appears to be a sex-related factor that affects the age of presentation. Bird et al, in their review of 291 parent-child pairings, found a much earlier onset and faster progression of HD in the children of male patients when compared with those of female parents (26). They also reported that when HD presents in the first 2 decades of life, the father is the affected parent 70% of the time. Reports of monozygotic Huntington twins, even separated at birth, who experienced clinical onset of HD at the same age (25) further support this notion of a sex-related factor affecting disease onset. In our series of six patients, four were associated with paternal lines of inheritance.

Genetically, HD has been linked to a locus within the terminal subband of the short arm of chromosome 4 (1, 3, 27–29). The HD gene contains an expanded and unstable DNA segment made up of repeating patterns of a polymorphic trinucleotide, CAG. Normally, there are 10 to 30 copies of this triplet at this locus; however, in HD patients, this segment is typically unstable and expanded to greater than 36 copies (27). There is a strong inverse correlation between the length of the CAG segment and the age of onset for this disorder (27–29). Instability in the length of the CAG repeats, furthermore, varies from tissue to tissue, with higher degrees of mosaicism found in affected regions such as the basal ganglia. Patients with juvenile HD typically have the highest CAG repeat lengths and more pronounced levels of somatic mosaicism. Recently, Telenius et al (27) demonstrated increased CAG lengths and mosaicism not only in the brain but also in the sperm of HD patients. They suggested that spermatogenesis may itself contribute to CAG expansion and may account for the tendency of earlier onset of HD in the offspring of male patients.

Juvenile HD has a different clinical presentation from that of its adult counterpart (3–10). Chorea, a distinctive early feature of adult HD, usually is a late manifestation in younger patients that eventually will be manifest in up to 66% to 90% of patients. In children with HD, cerebellar symptoms (50% to 100%), dyslalia (83% to 90%), mental deterioration (83% to 85%), and rigidity (65% to 83%) are the dominant protean initial features. Pediatric patients also may demonstrate seizure activity (33% to 67%), which typically is not encountered in the adult form. Because of the lack of the characteristic choreiform movement disorder initially, juvenile HD frequently presents a diagnostic dilemma, and the diagnosis usually is entertained only after a family history is elicited. The history of HD, as in our patients, is invariably very extensive.

The clinical course of HD in children, furthermore, often is more progressive. The average survival of juvenile patients is 7 to 8 years after onset versus 14 to 15 years as seen in adult patients (4, 6, 9, 26). Death results from complications related to chronic illness (4), most notably respiratory disease, as evidenced by our case 1, in which the child died at the age of 8 years secondary to cardiorespiratory arrest as a complication of an aspiration pneumonia.

Pathologically, HD is characterized by diffuse cerebral atrophy, which is most dramatic in the caudate nuclei and, to a lesser extent, the putamina (3–4, 6, 8, 10, 30). There is 2½ times more destruction of the basal ganglia than of the

remainder of the brain in HD (30). In pediatric HD patients, the globus pallidus and the cerebellum, areas not typically involved in adult patients, may be involved (4, 6, 8, 10). These regions of additional destruction may account for the rigidity and balance difficulties seen in juvenile HD but not in the adult form.

HD's preferential injury to the basal ganglia curiously is similar to that seen with metabolic derangements such as hypoxia and Leigh disease (31). The description of basal ganglia hypometabolism on positron emission tomography examinations (32–34) before bulk tissue loss and metabolic defects in respiratory chain complexes I and III/IV (35, 36) have led researchers to postulate a metabolic basis for HD. Recently, the abnormal metabolic regulation of glutamate, an excitotoxin, has been proposed as the mechanism for the cerebral damage in HD (37–41). More specifically, Perry and Hansen have suggested that the underlying cause of the neuronal destruction in HD was the toxic accumulation of glutamate secondary to its decreased reuptake from the receptor site (38).

The primary CT and MR feature of HD is caudate atrophy, which is best identified by separation of the horizontally apposed heads of the caudate nuclei (increased CC distance). A widened CC, however, is not specific for HD and also can be seen with hydrocephalus or other forms of diffuse atrophy. Because there is preferential caudate atrophy in HD, ratios comparing the intercaudate distance (CC) with internal standards (FH and IT, Fig 1) have been used to differentiate HD from other disorders (13–20). Recently, Aylward et al have shown by MR that both the FH/CC and bicaudate (CC/IT) ratios correlate well with caudate volume in patients with Huntington disease (23). No studies, however, have found good correlation of any ratios or measurements with the severity of clinical symptoms.

In any case, established criteria for HD are based primarily on adult data (normal mean FH/CC, 2.2 to 2.6; normal mean CC/IT, 0.09 to 0.12) (13–20, 23). Because the FH/CC ratio decreases with normal aging (15), presumably because ventricular size increases with age (42–44), the use of adult standards especially for the FH/CC would serve as conservative standards in children. In our series of healthy children, the mean FH/CC ratio (3.85 ± 1.35) was indeed higher than that reported in adults. The mean bicaudate ratio (0.093 ± 0.07), however, was comparable to reported adult values. Comparison of these normal FH/CC and bicaudate ratios in healthy children with that of our juvenile HD patients (Figs 4 and 5) demonstrated statistically significant differences between the two groups for both ratios.

Clinical symptoms, however, commonly predate CT findings, as was demonstrated in cases 1 and 2. MR, with the potential ability to detect subtle changes in the caudate nuclei and putamina as seen in cases 4 (Figs 2C–D), 5, and 6 (Figs 3B–C), may prove more helpful in the detection of early HD. Mirowitz et al, in their series of 65 pediatric patients with neurodegenerative disease, also had reported bilateral symmetric basal ganglia T2 hyperintensity in two patients with HD (24). Increased T2 signal has yet to be described in adult HD, to our knowledge.

Symmetric involvement of the basal ganglia, of course, is not limited to juvenile HD and may be found in a host of other conditions, many of which are metabolic in nature (31). The differential considerations include chronic disorders such as Leigh disease and Wilson disease. Acute hypoxia, carbon monoxide, hypoglycemia, and near drowning also may manifest bilateral basal ganglia lesions; however, with the clinical history of chronic symptoms, these causes should be easily discounted. The differentiation of juvenile HD from Leigh and Wilson diseases may be more difficult. Leigh (Fig 6) and Wilson diseases may have additional focal involvement of white matter, thalamus, brain stem, and cerebellum, whereas HD typically would not. Biochemically, patients with Leigh disease will have elevated lactate/pyruvate ratios and lactic acidosis; patients with Wilson disease, decreased serum ceruloplasmin and elevated urinary copper. Because these disorders are typically hereditary, a family history also would be helpful.

As demonstrated in our series, the FH/CC and bicaudate ratios, which can characterize preferential caudate atrophy, are useful radiologic measurements for the confirmation of HD in children. MR can potentially identify abnormalities not readily apparent with CT within the caudate nuclei and putamina in juvenile HD. The added use of the FH/CC and bicaudate ratios (Figs 4 and 5) can help differentiate HD from other neurodegenerative disorders, such as Leigh and Wilson diseases, which also may manifest bilateral basal ganglia abnormalities.

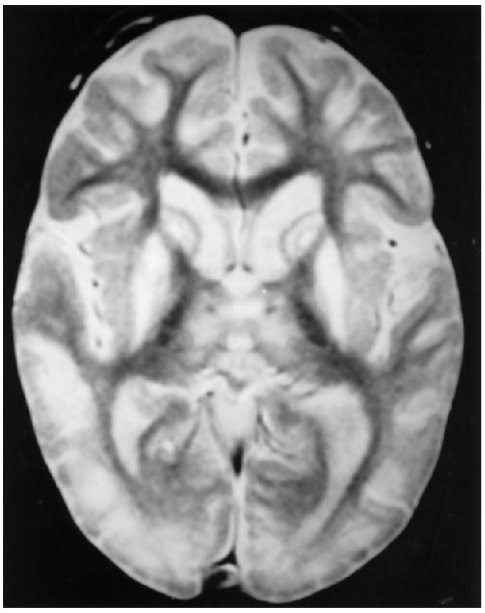

Fig 6. Leigh disease. Seven-year-old child with a long history of seizure, developmental delay, lactic acidosis, and dystonia. Axial T2-weighted MR image reveals hyperintensity in the caudate nuclei and putamina bilaterally (note that the caudate nuclei and putamina, however, are not atrophic; compare with Figures 2 and 3). There also was involvement of the thalami and subcortical white matter (from Ho et al [31]).

The presence of abnormal high signal intensity in atrophic caudate nuclei and putamina on proton density– and T2-weighted images in a child should suggest the diagnosis of Huntington disease.

References

1. Gusella JF, Wexler NS, Conneally PM, et al. A polymorphic DNA marker genetically linked to Huntington's disease. *Nature* 1983; 306:234–238
2. Shoulson I. Huntington's disease. *Neurol Clin* 1984;2:515–526
3. Martin JB, Gusella JF. Huntington's disease; pathogenesis and management. *N Engl J Med* 1986;315:1267–1276
4. Jervis GA. Huntington's chorea in childhood. *Arch Neurol* 1963; 9:244–257
5. Hansotia P, Cleeland CS, Chun RWM. Juvenile Huntington's chorea. *Neurology* 1968;18:217–224
6. Markham CH, Knox JW. Observations on Huntington's chorea in childhood. *J Pediatr* 1965;67:46–57
7. Byers RK, Dodge JA. Huntington's chorea in children: report of four cases. *Neurology* 1967;17:587–596
8. Byers RK, Gilles FH, Fung C. Huntington's disease in children: neuropathologic study of four cases. *Neurology* 1973;23:561–569
9. van Dijk JG, van der Velde EA, Roos RAC, Bruyn GW. Juvenile Huntington disease. *Hum Genet* 1986;73:235–239
10. Haslam RHA, Curry B, Johns R. Infantile Huntington's disease. *Can J Neurol Sci* 1983;10:200–203
11. Blinderman EE, Weidner W, Markham CH. The pneumoencephalogram in Huntington's chorea. *Neurology* 1964;14:601–607
12. Gath I, Vinje B. Pneumoencephalographic findings in Huntington's chorea. *Neurology* 1968;18:991–996
13. Terrence CF, Delaney JF, Alberts MC. Computed tomography for Huntington's disease. *Neuroradiology* 1977;13:173–175
14. Barr AN, Heinze WJ, Dobben GD, Valvassori GE, Sugar O. Bicaudate index in computerized tomography of Huntington disease and cerebral atrophy. *Neurology* 1978;28:1196–1200
15. Neophytides AN, Di Chiro G, Barron SA, Chase TN. Computed axial tomography in Huntington's disease and persons at-risk for Huntington's disease. *Adv Neurol* 1979;23:185–191
16. Oepen G, Ostertag C. Diagnostic value of CT in patients with Huntington's chorea and their offspring. *J Neurol* 1981;225:189–196
17. Stober T, Wussow W, Schimrigk K. Bicaudate diameter: the most specific and simple CT parameter in the diagnosis of Huntington's disease. *Neuroradiology* 1984;26:25–28
18. Lang C. Is direct CT caudatometry superior to indirect parameters in confirming Huntington's disease? *Neuroradiology* 1985;27: 161–163
19. Starkstein SE, Folstein SE, Brandt J, Pearlson GD, McDonnell A, Folstein M. Brain atrophy in Huntington's disease: a CT-scan study. *Neuroradiology* 1989;31:156–159
20. Sax D, O'Donnell B, Butters N, Menzer L, Montgomery K, Kayne HL. Computed tomographic, neurologic, and neurophysiological correlates of Huntington's disease. *Intern J Neuroscience* 1983; 18:21–36
21. Simmons JT, Pastakia B, Chase TN, Shults CW. Magnetic resonance imaging in Huntington disease. *AJNR Am J Neuroradiol* 1986;7:25–28
22. Rutledge JN, Hilal SK, Silver AJ, Defendini R, Fahn S. Study of movement disorders and brain iron by MR. *AJNR Am J Neuroradiol* 1987;8:397–411
23. Aylward EH, Schwartz J, Machlin S, Pearlson G. Bicaudate ratio as a measure of caudate volume on MR images. *AJNR Am J Neuroradiol* 1991;12:1217–1222
24. Mirowitz SA, Sartor K, Prensky AJ, Gado M, Hodges FJ. Neurodegenerative diseases of childhood: MR and CT evaluation. *J Comput Assist Tomogr* 1991;15:210–222
25. Sudarsky L, Myers RH, Walshe TM. Huntington's disease in monozygotic twins reared apart. *J Med Genet* 1983;20:408–411
26. Bird ED, Caro AJ, Pilling JB. A sex related factor in the inheritance of Huntington's chorea. *Ann Hum Genet* 1974;37:255–260
27. Telenius H, Kremer B, Goldberg YP, et al. Somatic and gonadal mosaicism of the Huntington disease gene CAG repeat in brain and sperm. *Nat Genet* 1994;6:409–414
28. Gusella JF, MacDonald ME, Ambrose CM, Duyao MP. Molecular genetics of Huntington's disease. *Arch Neurol* 1993;50:1157–1163
29. Gusella JF, MacDonald ME. Huntington's disease and repeating trinucleotides. *N Engl J Med* 1994;330:1450–1451
30. Bird ED. The brain in Huntington's chorea. *Psychol Med* 1978;8: 357–360
31. Ho VB, Fitz CR, Chuang SH, Geyer CA. Bilateral basal ganglia lesions: pediatric differential considerations. *Radiographics* 1993; 13:269–292
32. Kuhl DE, Phelps ME, Markham CH, Metter EJ, Riege WH, Winter J. Cerebral metabolism and atrophy in Huntington's disease determined by ^{18}FDG and computed tomographic scan. *Ann Neurol* 1982;12:425–434
33. Matthews PM, Evans AC, Andermann F, Hakim AM. Regional cerebral glucose metabolism differs in adult and rigid juvenile forms of Huntington disease. *Pediatr Neurol* 1989;5:353–356

34. Young AB, Penny JB, Starosta-Rubinstein S, et al. PET scan investigation of Huntington's disease: cerebral metabolic correlates of neurological features and functional decline. *Ann Neurol* 1986;20:296–303
35. Parker WD, Boyson SJ, Luder AS, Parks JK. Evidence for a defect in NADH:ubiquinone oxidoreductase (complex I) in Huntington's disease. *Neurology* 1990;40:1231–1234
36. Mann VM, Cooper JM, Javoy-Agid F, Agid Y, Jenner P, Schapira AHV. Mitochondrial function and parental sex effect in Huntington's disease. *Lancet* 1990;336:749
37. Beal MF, Kowall NW, Ellison DW, Mazurek MF, Swartz KJ, Martin JB. Replication of the neurochemical characteristics of Huntington's disease by quinolinic acid. *Nature* 1986;321:168–171
38. Perry TL, Hansen S. What excitotoxin kills striatal neurons in Huntington's disease? Clues from neurochemical studies. *Neurology* 1990;40:20–24
39. DiFiglia M. Excitotoxic injury of the neostriatum: a model for Huntington's disease. *Trends Neurosci* 1990;13:286–289
40. Albin RL, Young AB, Penney JB, et al. Abnormalities of striatal projection neurons and N-methyl-D-aspartate receptors in presymptomatic Huntington's disease. *N Engl J Med* 1990;322:1293–1298
41. Albin RL, Reiner A, Anderson KD, Penney JB, Young AB. Striatal and nigral neuron subpopulations in rigid Huntington's disease: implications for the functional anatomy of chorea and rigidity-akinesia. *Ann Neurol* 1990;27:357–365
42. Ford CV, Winter J. Computerized axial tomograms and dementia in elderly patients. *J Gerontol* 1981;36:164–169
43. Barron SA, Jacobs L, Kinkel WR. Changes in size of normal lateral ventricles during aging determined by computed tomography. *Neurology* 1976;26:1011–1013
44. Gyldensted C. Measurements of the normal ventricular system and hemispheric sulci of 100 adults with computed tomography. *Neuroradiology* 1977;14:183–192